

NRC Publications Archive Archives des publications du CNRC

Uniaxial compressive strength and deformation of Beaufort Sea ice Frederking, R. M. W.; Timco, G. W.

This publication could be one of several versions: author's original, accepted manuscript or the publisher's version. /
La version de cette publication peut être l'une des suivantes : la version prépublication de l'auteur, la version
acceptée du manuscrit ou la version de l'éditeur.

Publisher's version / Version de l'éditeur:

*The Seventh International Conference on Port and Ocean Engineering under
Arctic Conditions. POAC 83, 1, pp. 89-98, 1983*

NRC Publications Archive Record / Notice des Archives des publications du CNRC :
<https://nrc-publications.canada.ca/eng/view/object/?id=e11186d7-bab4-4825-ac8c-7e798f80b0c8>
<https://publications-cnrc.canada.ca/fra/voir/objet/?id=e11186d7-bab4-4825-ac8c-7e798f80b0c8>

Access and use of this website and the material on it are subject to the Terms and Conditions set forth at
<https://nrc-publications.canada.ca/eng/copyright>

READ THESE TERMS AND CONDITIONS CAREFULLY BEFORE USING THIS WEBSITE.

L'accès à ce site Web et l'utilisation de son contenu sont assujettis aux conditions présentées dans le site
<https://publications-cnrc.canada.ca/fra/droits>

LISEZ CES CONDITIONS ATTENTIVEMENT AVANT D'UTILISER CE SITE WEB.

Questions? Contact the NRC Publications Archive team at
PublicationsArchive-ArchivesPublications@nrc-cnrc.gc.ca. If you wish to email the authors directly, please see the
first page of the publication for their contact information.

Vous avez des questions? Nous pouvons vous aider. Pour communiquer directement avec un auteur, consultez la
première page de la revue dans laquelle son article a été publié afin de trouver ses coordonnées. Si vous n'arrivez
pas à les repérer, communiquez avec nous à PublicationsArchive-ArchivesPublications@nrc-cnrc.gc.ca.

Ser
TH1
N21d
o. 1150
c. 2
BLDG



National Research
Council Canada

Conseil national
de recherches Canada

**UNIAXIAL COMPRESSIVE STRENGTH AND DEFORMATION OF
BEAUFORT SEA ICE**

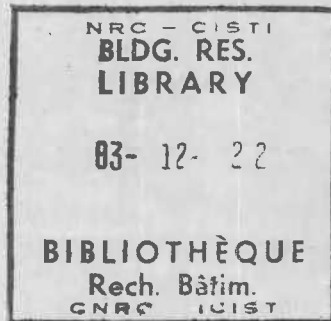
by R. Frederking and G.W. Timco

ANALYZED

Appeared in
VTT Symposium 27
The Seventh International Conference on Port and
Ocean Engineering under Arctic Conditions
Helsinki, Finland, 5 - 9 April, 1983
Volume 1, p. 89 - 98

Reprinted with permission
Technical Research Centre of Finland (VTT)

DBR Paper No. 1150
Division of Building Research



Price \$1.00

OTTAWA

NRCC 22805

RÉSUMÉ

Le comportement au point de vue des déformations et de la résistance d'échantillons de glace colonnaire granulaire orientés horizontalement a été mesuré in-situ. Les échantillons cylindriques ont été placés entre les plateaux d'une machine d'essai et les échantillons en forme de prisme entre des plateaux en acier de façon à obtenir différentes rigidités du mécanisme de la machine d'essai. Ce dernier a un effet non négligeable sur les mesures de résistance lorsque les résultats sont interprétés en fonction des taux de déformation nominale; mais, exprimés en taux de contraintes, cette influence a été presque totalement éliminée. La résistance de la glace granulaire (2,5 - 4 MPa) a été nettement supérieure à celle de la glace granulaire colonnaire (1 - 2,5 MPa). Mis à part la structure du grain, les échantillons se sont tous rompus lorsqu'ils ont subi des déformations de l'ordre de 10^{-3} .

CISTI / ICIST



3 1809 00210 3122

R. Frederking, Division of Building Research, National Research Council of Canada, Ottawa, Canada K1A 0R6.
G.W. Timco, Division of Mechanical Engineering, National Research Council of Canada, Ottawa, Canada K1A 0R6.

UNIAXIAL COMPRESSIVE STRENGTH AND DEFORMATION OF BEAUFORT SEA ICE

Abstract

Strength and deformation behaviour of horizontally oriented specimens of granular and columnar-grained ice were measured in the field. Cylindrical specimens were loaded on compliant platens and prismatic specimens on steel platens to provide a range of loading system stiffness. Loading system stiffness proved to have a significant effect on strength when the results were interpreted in terms of nominal strain rate, but in terms of stress rate it was largely eliminated. The strength of the granular ice (2.5 - 4 MPa) was substantially higher than that of columnar-grained ice (1 - 2.5 MPa). Regardless of grain structure, the specimens all failed by yielding at a strain of about 3×10^{-3} .

1 INTRODUCTION

Increasing interest in Arctic regions has resulted in expanding demands for knowledge of the mechanical properties of sea ice, information that is essential in establishing design ice loads on offshore structures and in transferring performance experience on existing structures to new locations. Measured mechanical properties are dependent on factors that can be divided into two categories the physical properties of the ice and the characteristics of the test system. Physical properties of ice include grain structure and size, temperature, salinity, porosity and air content. Test system characteristics include basic

stiffness of the loading frame, loading fixtures, and machine capacity. As has been pointed out by the IAHR Ice Testing Methods Working Group /1/, it is necessary to document as completely as possible all factors affecting measured results.

2 SAMPLE ACQUISITION AND SPECIMEN PREPARATION

The ice used in this study was cut 6 January 1982 from a rafted block (~ 5 m × 5 m × 0.8 m thick) in a rubble field about 20 m to the west of Tarsiut, a caisson-retained island about 40 km offshore in the Beaufort Sea. The rubble had formed 4 January 1982 so that the ice had only recently been exposed. Mean air temperature was about -35°C. Further details of sample acquisition and transportation are described in a companion paper in these proceedings /3/.

The upper 30 cm of the ice cover comprised granular ice with a grain size increasing from 1 mm at the top to 3 mm at a depth of 30 cm. The lower 50 cm of the ice cover comprised columnar grains of 5 to 10 mm. A more complete description of the physical characteristics of the ice is available /4/. Horizontal cores 7.56 cm in diameter were taken from depths of 15-20 cm (top specimens) and 60-65 cm (bottom specimens) to make cylindrical specimens for uniaxial compression tests. The ice in the top specimens showed a discontinuous columnar structure, with columnar grains about 1 cm long and 1-3 mm in diameter. Columnar ice in the bottom specimens (grain diameter 8 mm) showed a tendency for a preferred azimuthal orientation of the c-axis in the horizontal plane at an angle of about 30 deg to the axis of the specimen.

Cylindrical specimens 23, 20, 15 and 10 cm long were cut to optimize use of the available pieces of core. No further end preparation, other than brushing off loose snow, was carried out. A set of 10 prismatic specimens from seven different levels in the ice was prepared for uniaxial compression tests. They were

19.2 cm long by 5.5 cm wide by 5.1 cm thick and the ends were smoothed with fine emery paper to provide a polished flat surface. Salinity was in the range $4.5 \pm 5\%$, and ice density was $900 \pm 10 \text{ kg/m}^3$.

3 TEST PROCEDURE

Testing was carried out on a motorized 0.05 MN capacity compression tester (Soiltest CT-405), a screw-drive machine with actuator rates in the range 0.2 to 4 mm/min. "Maraset" compliant platens were used to eliminate the effect of irregularities and to reduce radial stresses at the ends of the cylindrical specimens. Two extensometers were fixed directly to the specimen, their output averaged to obtain strain. Continuous records of load versus time and displacement versus time were made. A typical record is presented in Figure 1, and definitions of yield stress, σ , loading stress rate, $\dot{\sigma}_l$, average stress rate, $\dot{\sigma}_{av}$, strain at yield, ϵ_y , and strain rate at yield, $\dot{\epsilon}_y$, are

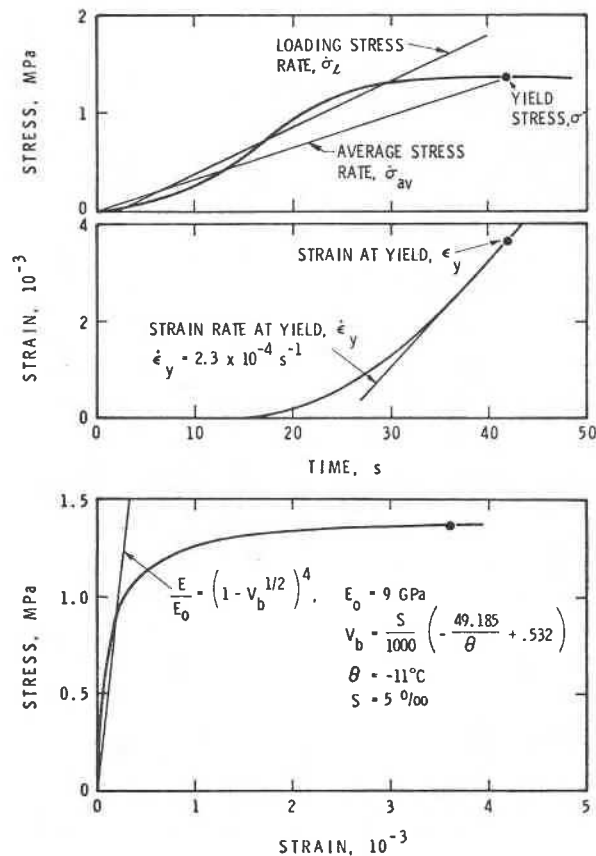


Figure 1. Stress-time and strain-time curves for test 1 on cylindrical specimen: $\dot{\epsilon}_{nom} = 2 \times 10^{-4} \text{ s}^{-1}$, test temperature -11°C

illustrated. Nominal strain rate, $\dot{\epsilon}_{nom}$, is nominal machine speed divided by specimen length. The prism specimens were loaded on steel platens to obtain a stiffer loading system. Before testing, all specimens were stored in a chest freezer at $-11 \pm 1^\circ\text{C}$.

4 TEST RESULTS AND DISCUSSION

Complete test results are tabulated in Table 1, and strength versus loading stress rate is plotted in Figure 2. The results from the top and bottom cores fall into distinctly different groups that can be related to grain structure. The larger-grained bottom specimens, with preferred c-axis orientation at 30 deg to the specimen axis, had half the strength of the more granular top specimens when tested at comparable stress rates. Also presented on Figure 2 are strength results at a single nominal strain rate of $2 \times 10^{-4} \text{ s}^{-1}$ for prism specimens at different levels in the ice cover; the number in brackets following each datum point represents the average depth (in cm) of each specimen. It may be seen that the test results for the prism specimens in the upper part of the ice cover agree with the values for the top cylinders. Similarly, the prisms at depths between 40 and 60 cm have strengths similar to those of the bottom cylinders. Specimens at depths of 23 and 29 cm, where

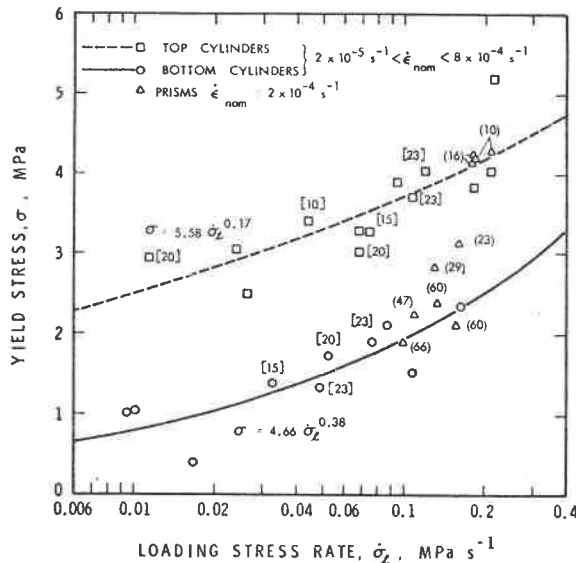


Figure 2. Uniaxial compressive strength of horizontally Beaufort Sea, -11°C . () Depth in cm of prism specimens; [] Length in cm of cylindrical specimens

grain structure is columnar but grain size smaller than at greater depths, have strengths intermediate between those of the top and bottom cylinders. This points to the importance of grain

TABLE 1 Uniaxial Compression Data Test Temperature: $-11^{\circ} \pm 1^{\circ}\text{C}$

Test No.	Yield Stress MPa	Loading Stress Rate kPa s ⁻¹	Strain at Yield x 10 ³	Time to Yield s	Strain Rate at Yield s ⁻¹ x 10 ⁴	Nominal Strain Rate s ⁻¹ x 10 ⁴
<u>Cylindrical Specimens</u>						
1-23*-B**	1.37	49	3.7	42	2.3	2
2-23-B	1.92	77	2.0	35	1.8	2
3-23-T	4.04	120	2.5	46	2.0	2
4-23-T	3.71	110	3.6	48	2.1	2
5-20-T	4.04	210	2.9	24	3.8	4
6-20-B	1.55	110	-	21	-	4
7-20-T	3.02	68	0.1	58	1.2	2
8-20-B	1.74	53	2.4	49	1.5	2
9-20-T	2.51	26	0.9	153	0.59	0.8
10-20-B	1.04	9.5	0.5	186	0.26	0.4
11-20-T	2.95	11	2.4	342	0.35	0.2
12-15-T	3.85	180	4.6	27	4.6	5
13-15-B	2.38	160	2.2	22	4.6	5
14-15-B	2.14	87	4.0	38	2.6	3.5
15-15-T	3.30	68	2.7	64	1.3	2
16-15-B	1.39	32	3.0	66	1.8	2
17-15-B	1.07	10	6.5	180	0.57	0.8
18-15-T	3.04	24	2.1	174	0.46	0.8
19-10-T	5.22	220	-	30	-	8
20-10-T	3.91	95	-	57	-	3.5
21-10-T	3.41	45	-	108	-	2
22-15-T***	3.28	75	0.2	71	1.3×10^{-4}	2
23-15-B***	0.415	17	2.3	41	1.6×10^{-4}	2
<u>Prism Specimens</u>						
4-29 ⁺	2.84	131	-	34	-	2
4-16	4.26	181	-	33	-	2
1-16	4.17	183	-	36	-	2
6-47	2.27	110	-	44	-	2
6-66	1.88	103	-	30	-	2
1-60	2.29	133	-	26	-	2
6-60	2.13	156	-	23	-	2
3-10	4.21	186	-	36	-	2
2-10	4.30	215	-	28	-	2
3-23	3.13	158	-	30	-	2

* Specimen length, cm; ** B for bottom specimens, T for top specimens; ***No compliant platen; ⁺ Mean depth of specimen in ice cover, cm

structure and grain size in determining strength. It is also noteworthy that strength results, on a stress rate basis, are quite similar for simply prepared specimens on compliant platens and finely prepared prism specimens on steel platens.

A power function can be fitted to the strength versus loading stress rate results. The expression for the top specimens (granular ice) is

$$\sigma = 5.58 \dot{\sigma}_\ell^{0.17} \quad (1)$$

with a correlation coefficient $r^2 = 0.63$. The expression for the bottom specimens (columnar ice) is

$$\sigma = 4.66 \dot{\sigma}_\ell^{0.38} \quad (2)$$

with a correlation coefficient $r^2 = 0.74$. In both equations (1) and (2) σ has units of MPa and $\dot{\sigma}_\ell$ MPa s⁻¹. These strength equations can be expressed in terms of average stress rate $\dot{\sigma}_{av}$ using the relation

$$\dot{\sigma}_\ell = 1.31 \dot{\sigma}_{av}^{0.96} \quad (3)$$

with a correlation coefficient $r^2 = 0.99$. Equation (3) is determined from the stress rate data of all the top and bottom specimens presented in Table 1 and can be used to convert equations (1) and (2) from a loading stress rate basis to an average stress rate basis. The reader should be cautioned not to extrapolate the preceding or following empirical equations beyond the range of the experimental data; such extrapolation could lead to absurd conclusions.

Expressing yield stress of columnar-grained ice in terms of average stress rate gives

$$\sigma = 5.16 \dot{\sigma}_{av}^{0.36} \quad (4)$$

This compares with results of tests on horizontally oriented specimens of columnar-grained first-year sea ice from Pond Inlet and Mould Bay which gave /2/

$$\sigma = 4.47 \dot{\sigma}_{av}^{0.28} \quad (5)$$

A number of factors such as grain size and orientation, specimen preparation, test machine, etc., differ (between the two data sources, equations (4) and (5)), but over the average stress rate range of 10⁻² to 10⁻¹ MPa s⁻¹ strength results are comparable.

It has been pointed out that the strength results can be examined in terms of time to yield or failure in order to verify the satisfactory performance of a test machine /2/. This has been done in Fig. 3, which shows that there is a trend towards decreasing time to yield with increasing strength, as would be expected. The curves drawn through the datum points are regression lines, but since the correlation coefficients were quite low, no equations are presented.

In Figure 1 it may be seen that although the test was run at a constant nominal strain rate of $2 \times 10^{-4} \text{ s}^{-1}$, strain rate is far from constant. Over the range of 10^{-5} s^{-1} to 10^{-4} s^{-1} the strain rate at yield is about 70% of the nominal strain rate. Also shown (Figure 1c) is a line representing the dynamic elastic modulus determined from brine volume /5/. The higher measured slope at very small strains suggests experimental error in the strain measurements.

Space limitations preclude plotting the strength results on a strain rate basis, but close examination of the data in Table 1 indicates that at a given nominal strain rate there is a significant difference in strength for compliant and steel platens. At a nominal strain rate of $2 \times 10^{-4} \text{ s}^{-1}$ the strengths of granular ice were 3.4 and 4.0 MPa for compliant and steel

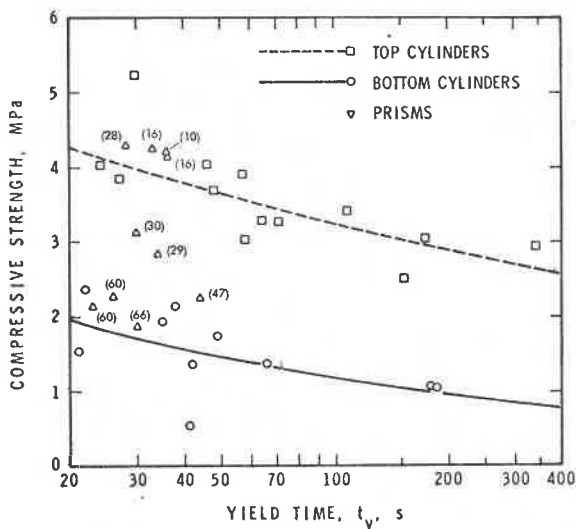


Figure 3. Uniaxial compressive strength vs time to yield of first-year sea ice from the Beaufort Sea, -11°C . () Depth in cm of prism specimens

platens, respectively, and for columnar ice, 1.6 and 2.1 MPa. Differences can be explained in terms of test system stiffness.

The results for cylindrical specimens were examined to determine the effect of specimen length at the nominal strain rate of $2 \times 10^{-4} \text{ s}^{-1}$, but no systematic influence could be established. On the other hand, plotting results on a stress rate basis (see datum points in square brackets, Fig. 2) confirmed the pattern of increasing strength with increasing stress rate. Examination of yield strain and strength showed considerable scatter, with no apparent relation between them. The average strain at yield was $2.75 \pm 1.35 \times 10^{-3}$ for all the specimens; there was no significant difference between granular and columnar ice.

An investigation was also made of the stiffness of the test machine and loading system. Stiffness for the whole system can be quite different from that of the basic test machine owing to the influence of the load cell, platens, alignment joints, etc. The characteristics of the system were therefore determined by loading a specimen of known constant elasticity and measuring the load, movement of the screw jack, and load frame deflection. The test machine, its components, and the points between which deflections were measured are shown in Figure 4a (a schematic of the specimen and loading system is presented in Figure 4b).

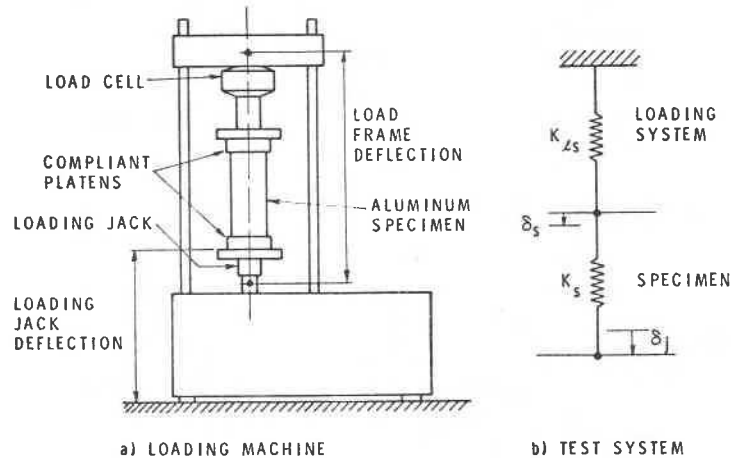


Figure 4. Schematics of arrangements for determining loading system stiffness

Loading system stiffness, $K_{\ell s}$, is defined as

$$K_{\ell s} = \frac{\Delta P}{\delta_j - \delta_s} \quad (6)$$

where ΔP is a load increment, δ_j is the corresponding displacement increment of the screw jack, and δ_s is the resulting deformation increment of the specimen. δ_s is defined as

$$\delta_s = \frac{\Delta P \ell}{E A} \quad (7)$$

where E is the elastic modulus of the specimen, ℓ is its length, and A its cross-sectional area. Substituting equation (7) in (6), the following equation for determining loading system stiffness is obtained

$$K_{\ell s} = \frac{\Delta P}{\delta_j \frac{\Delta P \ell}{E A}} \quad (8)$$

Tests were conducted in a cold room at -15°C with an aluminum specimen ($\ell = 200$ mm, diameter = 76.2 mm, and $E = 70$ GPa) and compliant platens. The basic frame stiffness measured between the upper cross-head and screw-drive jack was about 200×10^6 N/m. The actual stiffness of the loading system, as calculated from equation (8) and measurements of load and screw-jack displacement, is presented in Figure 5. It may be seen that the stiffness of the loading system with compliant platens is not a constant, but a function of load and rate; loading system stiffness is substantially less than load frame stiffness. In tests with the aluminum specimen between steel platens, loading system stiffness was nearly constant (100 MN/m) for loads up to 0.06 MN.

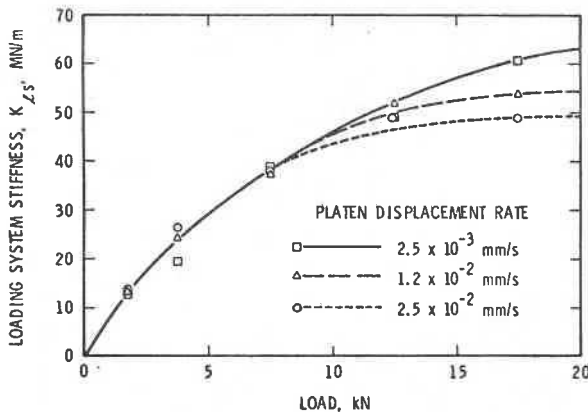


Figure 5. Loading system stiffness with compliant platens as a function of load and platen displacement rate, CT 405 test machine at -15°C

Direct application of loading system stiffness to the interpretation of these test results is beyond the scope of this paper. It may be seen, however, that for a given nominal strain rate a stiffer loading system will impose higher stress rates on a specimen. This could explain the higher strengths measured for prism specimens on steel platens (high loading system stiffness) than for cylindrical specimens on compliant platens (low loading system stiffness) at a given nominal strain rate of $2 \times 10^{-4} \text{ s}^{-1}$.

ACKNOWLEDGEMENTS

The authors would like to thank Gulf Resources Canada and Dome Petroleum for the opportunity to perform these experiments. The logistics, transportation and accommodation provided made the test program possible. The assistance of J. Neil in reducing the data and Mohamed Sayed in determining the test system stiffness is gratefully acknowledged. This paper is a contribution from both the Division of Building Research and Division of Mechanical Engineering, National Research Council Canada.

REFERENCES

1. IAHR Working Group on Standardizing Testing Methods in Ice, Standardized Testing Methods for Measuring Mechanical Properties of Ice. Journal of Cold Regions Science and Technology 4(1981), pp. 245-253.
2. Sinha, N.K., Field test 1 of compressive strength of first-year sea ice. Presented to Second Symposium on Applied Glaciology, West Lebanon, N.H., 1982. To be published in Annals of Glaciology.
3. Timco, G.W., and Frederking, R., Confined compressive strength of sea ice. The 7th Int. Conf. on Port and Ocean Engineering under Arctic Conditions (POAC). Helsinki 1983.
4. Timco, G.W., and Frederking, R., Flexural strength and fracture toughness of sea ice. Accepted for publication in Journal of Cold Regions Science and Technology 1982.
5. Weeks, W.F., and Assur, A., The mechanical properties of sea ice. Hanover, 1967. CRREL (Cold Regions Research and Engineering Laboratory) Cold Regions Science and Engineering Monograph, Pt. 2, Sec. C3.

This publication is being distributed by the Division of Building Research of the National Research Council of Canada. It should not be reproduced in whole or in part without permission of the original publisher. The Division would be glad to be of assistance in obtaining such permission.

Publications of the Division may be obtained by mailing the appropriate remittance (a Bank, Express, or Post Office Money Order, or a cheque, made payable to the Receiver General of Canada, credit NRC) to the National Research Council of Canada, Ottawa. K1A 0R6. Stamps are not acceptable.

A list of all publications of the Division is available and may be obtained from the Publications Section, Division of Building Research, National Research Council of Canada, Ottawa. K1A 0R6.